

1.9 μm waveguide laser fabricated by ultrafast laser inscription in $\text{Tm}:\text{Lu}_2\text{O}_3$ ceramic

J. MORRIS,^{1,2,*} N. K. STEVENSON,^{1,3} H. T. BOOKEY,¹ A. K. KAR,² C. T. A. BROWN,³ J.-M. HOPKINS,¹ M. D. DAWSON,^{1,4} AND A. A. LAGATSKY¹

¹Fraunhofer Centre for Applied Photonics, Fraunhofer UK, Technology and Innovation Centre, Glasgow, G1 1RD, UK

²School of Engineering and Physical Science, David Brewster Building, Heriot-Watt University, Edinburgh, EH14 4AS, UK

³SUPA, School of Physics and Astronomy, University of St Andrews, St Andrews, KY16 9SS, UK

⁴Institute of Photonics, University of Strathclyde, Technology and Innovation Centre, Glasgow, G1 1RD, UK

*jm510@hw.ac.uk

Abstract: The ultrafast laser inscription technique has been used to fabricate channel waveguides in Tm^{3+} -doped Lu_2O_3 ceramic gain medium for the first time to our knowledge. Laser operation has been demonstrated using a monolithic microchip cavity with a continuous-wave Ti:sapphire pump source at 796 nm. The maximum output power achieved from the $\text{Tm}:\text{Lu}_2\text{O}_3$ waveguide laser was 81 mW at 1942 nm. A maximum slope efficiency of 9.5% was measured with the laser thresholds observed to be in the range of 50–200 mW of absorbed pump power. Propagation losses for this waveguide structure are calculated to be $0.7 \text{ dB}\cdot\text{cm}^{-1} \pm 0.3 \text{ dB}\cdot\text{cm}^{-1}$ at the lasing wavelength.

© 2017 Optical Society of America

OCIS codes: (140.5680) Rare earth and transition metal solid-state lasers; (230.7370) Waveguides; (130.3120) Integrated optics devices; (140.3390) Laser materials processing.

References and links

1. R. R. Gattass and E. Mazur, "Femtosecond laser micromachining in transparent materials," *Nat. Photonics* **2**(4), 219–225 (2008).
2. D. Choudhury, J. R. Macdonald, and A. K. Kar, "Ultrafast laser inscription: perspectives on future integrated applications," *Laser Photonics Rev.* **8**(6), 827–846 (2014).
3. F. Chen and J. R. V. de Aldana, "Optical waveguides in crystalline dielectric materials produced by femtosecond-laser micromachining," *Laser Photonics Rev.* **8**(2), 251–275 (2014).
4. F. Fusari, R. R. Thomson, G. Jose, F. M. Bain, A. A. Lagatsky, N. D. Psaila, A. K. Kar, A. Jha, W. Sibbett, and C. T. Brown, "Lasing action at around 1.9 μm from an ultrafast laser inscribed Tm-doped glass waveguide," *Opt. Lett.* **36**(9), 1566–1568 (2011).
5. D. G. Lancaster, S. Gross, H. Ebendorff-Heidepriem, K. Kuan, T. M. Monro, M. Ams, A. Fuerbach, and M. J. Withford, "Fifty percent internal slope efficiency femtosecond direct-written $\text{Tm}^{3+}:\text{ZBLAN}$ waveguide laser," *Opt. Lett.* **36**(9), 1587–1589 (2011).
6. D. G. Lancaster, S. Gross, H. Ebendorff-Heidepriem, A. Fuerbach, M. J. Withford, and T. M. Monro, "2.1 μm waveguide laser fabricated by femtosecond laser direct-writing in Ho^{3+} , $\text{Tm}^{3+}:\text{ZBLAN}$ glass," *Opt. Lett.* **37**(6), 996–998 (2012).
7. Y. Ren, G. Brown, A. Ródenas, S. Beecher, F. Chen, and A. K. Kar, "Mid-infrared waveguide lasers in rare-earth-doped YAG," *Opt. Lett.* **37**(16), 3339–3341 (2012).
8. J. R. Macdonald, S. J. Beecher, P. A. Berry, G. Brown, K. L. Schepler, and A. K. Kar, "Efficient mid-infrared Cr:ZnSe channel waveguide laser operating at 2486 nm," *Opt. Lett.* **38**(13), 2194–2196 (2013).
9. C. Kränkel, "Rare-Earth-Doped Sesquioxides for Diode-Pumped High-Power Lasers in the 1-, 2-, and 3- μm Spectral Range," *IEEE J. Sel. Top. Quantum Electron.* **21**(1), 250–262 (2015).
10. S. M. Lima, T. Catunda, R. Lebullenger, A. C. Hernandes, M. L. Baesso, A. C. Bento, and L. C. M. Miranda, "Temperature dependence of thermo-optical properties of fluoride glasses determined by thermal lens spectrometry," *Phys. Rev. B* **60**(22), 15173–15178 (1999).
11. P. Koopmann, S. Lamrini, K. Scholle, P. Fuhrberg, K. Petermann, and G. Huber, "Efficient diode-pumped laser operation of $\text{Tm}:\text{Lu}_2\text{O}_3$ around 2 μm ," *Opt. Lett.* **36**(6), 948–950 (2011).
12. A. A. Lagatsky, O. L. Antipov, and W. Sibbett, "Broadly tunable femtosecond $\text{Tm}:\text{Lu}_2\text{O}_3$ ceramic laser operating around 2070 nm," *Opt. Express* **20**(17), 19349–19354 (2012).
13. E. V. Ivakin, I. G. Kisialiou, and O. L. Antipov, "Laser ceramics $\text{Tm}:\text{Lu}_2\text{O}_3$. Thermal, thermo-optical, and spectroscopic properties," *Opt. Mater.* **35**(3), 499–503 (2013).

14. A. Ikesue, Y. L. Aung, T. Taira, T. Kamimura, K. Yoshida, and G. L. Messing, "Progress in ceramic lasers," *Annu. Rev. Mater. Res.* **36**(1), 397–429 (2006).
15. A. Ikesue and Y. L. Aung, "Synthesis and performance of advanced ceramic lasers," *J. Am. Ceram. Soc.* **89**(6), 1936–1944 (2006).
16. O. L. Antipov, A. A. Novikov, N. G. Zakharov, and A. P. Zinoviev, "Optical properties and efficient laser oscillation at 2066 nm of novel Tm:Lu₂O₃ ceramics," *Opt. Mater. Express* **2**(2), 183–189 (2012).
17. D. P. Shepherd, A. Choudhary, A. A. Lagatsky, P. Kannan, S. J. Beecher, R. W. Eason, J. I. Mackenzie, X. Feng, W. Sibbett, and C. T. A. Brown, "Ultrafast High-Repetition-Rate Waveguide Lasers," *IEEE J. Sel. Top. Quantum Electron.* **22**(2), 16–24 (2016).
18. R. Yingying, G. Brown, R. Mary, G. Demetriou, D. Popa, F. Torrisi, A. C. Ferrari, C. Feng, and A. K. Kar, "7.8-GHz Graphene-Based Monolithic Waveguide Laser," *IEEE J. Sel. Top. Quantum Electron.* **21**(1), 395–400 (2015).
19. B. M. Walsh, "Review of Tm and Ho materials; spectroscopy and lasers," *Laser Phys.* **19**(4), 855–866 (2009).
20. S. Juodkakis, H. Misawa, and I. Maksimov, "Thermal accumulation effect in three-dimensional recording by picosecond pulses," *Appl. Phys. Lett.* **85**(22), 5239–5241 (2004).
21. J. A. Caird, S. A. Payne, P. R. Staber, A. J. Ramponi, L. L. Chase, and W. F. Krupke, "Quantum electronic properties of the Na₃Ga₂Li₃F₁₂: Cr³⁺ laser," *IEEE J. Quantum Electron.* **24**(6), 1077–1099 (1988).
22. R. Mary, S. J. Beecher, G. Brown, R. R. Thomson, D. Jaque, S. Ohara, and A. K. Kar, "Compact, highly efficient ytterbium doped bismuthate glass waveguide laser," *Opt. Lett.* **37**(10), 1691–1693 (2012).

1. Introduction

Ultrafast laser inscription (ULI) is now widely used for the fabrication of three dimensional photonic structures across a broad range of transparent dielectrics [1]. In ULI, when ultrashort (hundreds of fs to a few ps) laser pulses are tightly focused beneath the surface of a transparent dielectric material, nonlinear processes such as multi-photon absorption and/or tunneling ionization take place inducing avalanche ionization within the small focal volume of micron dimensions which leads to high temperatures and pressures through an induced micro-plasma. This imprints a permanent change in the structure and refractive index of the optical material. Depending on both the dielectric material properties and the inscribing laser parameters the refractive index change (Δn) inside the modified tracks could reach different values and signs leading to different types of waveguide structures [2]. Namely, in Type I waveguides ($\Delta n > 0$) the waveguide core is located inside the modified region. Type II structures ($\Delta n < 0$) support guiding between two modified tracks through the stress induced refractive index modification effect. Furthermore, a waveguide core can be formed inside the unmodified material region which is surrounded by a number of a lower index inscribed tracks ($\Delta n < 0$) referred to as a depressed cladding structure. ULI has several advantages over lithographic methods used to produce planar and ridge waveguides such as single step and rapid fabrication, three dimensional design freedom and applicability to a wide range of crystalline and amorphous materials.

To date, a wide range of compact and highly-efficient solid-state laser sources have been demonstrated based on ULI waveguide structures fabricated in rare-earth (RE) and transition-metal ion doped crystalline, ceramic and glass gain media [2, 3]. Considering the mid-infrared (mid-IR) region (around 2 μm and beyond), channel waveguide lasers have been realized predominantly in Tm-/Ho-doped glasses (at $\sim 1.9 - 2.05 \mu\text{m}$ and $2.9 \mu\text{m}$), where high efficiencies have been demonstrated utilizing the depressed cladding structures [4–6]. To date, the work on the mid-IR waveguide lasers written in crystalline or ceramic gain media is limited to a few demonstrations, namely, Tm-doped YAG ceramic, producing up to 90 mW at around 2 μm [7] and Cr-doped ZnSe generating 285 mW at 2.5 μm [8] using depressed cladding geometries in both cases.

Previously, a family of laser hosts known as sesquioxides, RE₂O₃ (RE = Y, Sc, and Lu), have been shown to demonstrate efficient, high-power and tunable laser operation around the 2 μm region in both continuous-wave (CW) and pulsed regimes when doped with the Tm³⁺ or Ho³⁺ ions [9]. In particular, the Tm:Lu₂O₃ gain medium possesses beneficial thermo-optical properties such as high thermal conductivity (12.5 W/m·K) which outperforms the likes of ZBLAN (0.7–0.8 W/m·K) [10] and YAG (~ 7 W/m·K) at high doping concentrations, and a broad gain spectrum which covers >300 nm and extends well beyond 2 μm . These inherent

properties of Tm:Lu₂O₃ have led to the demonstration of 75 W of CW laser output around 2 μ m with a tuning range of >200 nm under direct laser diode pumping [11]. Moreover, the broad gain spectrum of Tm:Lu₂O₃ has allowed for the generation of 180 fs pulses from a modelocked source which also demonstrated sub 400 fs pulses with a center wavelength tunable over a 70 nm range [12].

Furthermore, due to the cubic lattice symmetry of Lu₂O₃ and other sesquioxides they can be fabricated in the form of laser ceramics [13] that offers a potential for size scalability and cost effective production. Laser ceramic manufacturing involves the cold, high pressure pressing of a powder filled mold of a desired shape followed by sintering under vacuum for a number of hours to form the ceramic sample and then final processing and polishing [14]. This process of producing sesquioxides laser elements has the advantage over the Heat-Exchanger or Nacken-Kyropoulos methods in that it has a shorter manufacturing time and requires a lower temperature whilst still being able to closely match the physical properties and laser performance demonstrated with single crystals [15, 16].

Combining the unique Tm:Lu₂O₃ optical properties with the ULI waveguide laser geometry would provide a means to produce compact, low-threshold and efficient laser sources near 2 μ m with the potential for high pulse repetition rate ultrafast operation [17, 18]. It makes such laser sources also compatible with chip technology that will create new opportunities in mid-IR sensing and metrology, medical applications [19] and as compact pumps for mid-IR supercontinuum generation. Here we report, for the first time to our knowledge, the demonstration of optical waveguides in a bulk Tm:Lu₂O₃ ceramic gain medium fabricated by ULI. Waveguide laser operation at 1942 nm was successfully demonstrated with an output power of up to 81 mW.

2. Waveguide fabrication and passive testing

As stated above, the type of waveguide which can be produced by ULI is heavily dependent on the material properties of the substrate and the inscribing laser parameters. In order to explore the range of induced refractive index change in Tm:Lu₂O₃ ceramic, arrays of 10 mm long tracks were fabricated using different pulse energies and track separations. The arrays were fabricated in a 2.3 \times 5 \times 10 mm sample of 1 at.% Tm³⁺-doped Lu₂O₃ ceramic (Konoshima Chemicals). Comparison of the Tm:Lu₂O₃ sample absorption spectra with the previously reported results [16] confirms that the doping concentration is within 1 at.% range (effective absorption coefficient of 0.68 cm⁻¹ at 796 nm).

The ultrafast laser used for waveguide writing (PHAROS, Light Conversion) emitted 200 fs pulses at a 500 kHz pulse repetition rate at a center wavelength of 1040 nm. All the waveguides were written 300 μ m beneath the sample surface using circularly polarized light focused with a 0.4 NA aspheric lens giving a spot diameter of approximately 1.8 μ m. The transverse writing geometry was selected for waveguide fabrication with a constant 5 mm/s translation speed. Due to the thermal diffusivity of Tm:Lu₂O₃ and the focal spot diameter used in the ULI process the waveguides were fabricated in the non-thermal regime, as given by [20]:

$$f_{cr} = \frac{D_{th}}{d^2} \quad (1)$$

where f_{cr} is the critical frequency where the time between pulses matches the heat diffusion time from the focal volume, D_{th} is the thermal diffusivity of the material and d is the focal spot diameter. Using the known spot size and thermal properties of Tm:Lu₂O₃ [9] we estimate the critical frequency to be approximately 1.7 MHz.

Waveguide depth was selected to avoid surface ablation during writing and with consideration of the working distance of the objective and the sample thickness. The writing speed was chosen taking into account capabilities of translation stages, writing time, and

ensuring good overlap of the pulses in the sample during writing. The pulse energy across the waveguide arrays was varied from 0.4 - 5 μJ with track separations of 20 μm and 30 μm . After the fabrication process the sample end facets were ground back to remove any defects caused by clipping of the inscription beam near the sample edges and re-polished to optical quality giving a final waveguide length of 9 mm.

An initial study of the guiding characteristics of the arrays was undertaken with a 980 nm fiber coupled diode laser using the setup depicted in Fig. 1(a). The fiber output beam was collimated using an aspheric lens with a focal length of 2.75 mm and then coupled into the waveguides using another aspheric lens with an 11 mm focal length resulting in a spot diameter size of 24 μm .

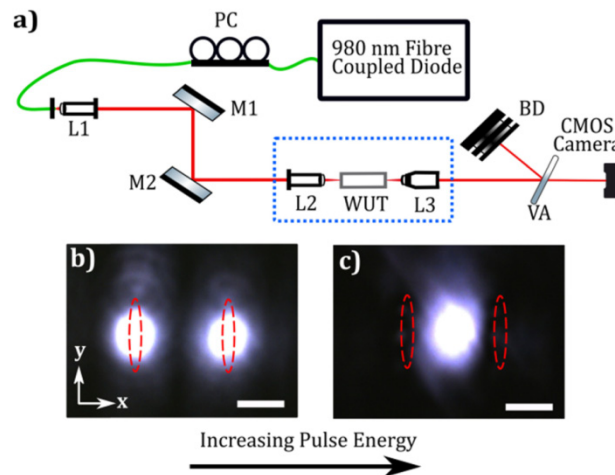


Fig. 1. (a) Experimental setup for initial waveguide characterization. PC, three paddle fiber polarization controller; L1 and L2, AR-coated aspheric lenses; M1 and M2, silver mirrors; WUT, waveguide under test; L3, $\times 20$ objective; VA, reflective variable ND filter; BD, beam dump. Blue dotted box signifies components mounted on waveguide alignment workstation. (b) and (c) Mode images for Type I and II guiding in $\text{Tm:Lu}_2\text{O}_3$ waveguides with 20 μm track separations, respectively. Red dashed ellipses indicate the area of the inscribed tracks. A 10 μm scale bar is included.

Type I guiding was observed for the track waveguides written with pulse energies from 0.4 – 0.8 μJ , where the guiding mode overlaps with the modified region [Fig. 1(b)]. This was confirmed by simultaneously coupling into both modification lines in a track waveguide and comparing the guiding region spacing with the known track separation. Type II guiding [Fig. 1(c)] was observed in the structures inscribed at pulse energies between 0.9 – 3 μJ . In this pulse energy range the tracks with separations of 20 μm were found to support single mode guiding at 980 nm, whereas the 30 μm separated tracks were found to be multimode. Structures inscribed with pulse energies >3 μJ were found to have limited guiding capabilities due to large material damage features. Also guiding in the Type II regime was found to be strongly polarization dependent with only light polarized parallel to the y-axis guided. The stress induced in the irradiated tracks during the inscription process, which enables Type II guiding, and the asymmetry of the track waveguide design is the likely cause of the strong polarization dependence.

3. Waveguide laser results

In order to test the potential for lasing from the inscribed waveguides, a cavity was formed around the sample using two plane dielectric mirrors mounted up against the uncoated 2.3×5 mm end facets, as shown in Fig. 2. The input pump mirror (PM) was coated for a high reflectivity in the range of 1.9 – 2.1 μm and a high transmission at the pump wavelength of

796 nm, whereas the output couplers (OC) with transmission of 2%, 9%, 20%, 30%, 40% and 75% between 1.9 – 2.1 μm were used, forming a standing wave cavity. The pump source was a tunable Ti:sapphire laser producing linearly polarized light with a maximum output power of 2 W at 796 nm. The slightly astigmatic pump beam was coupled into the waveguides using an aspheric lens with a 20 mm focal length resulting in an average diameter spot size of 27.5 μm . In order to thermally stabilize the cavity the mounting bracket for the sample was water cooled keeping the sample mount at a constant temperature of 20 °C.

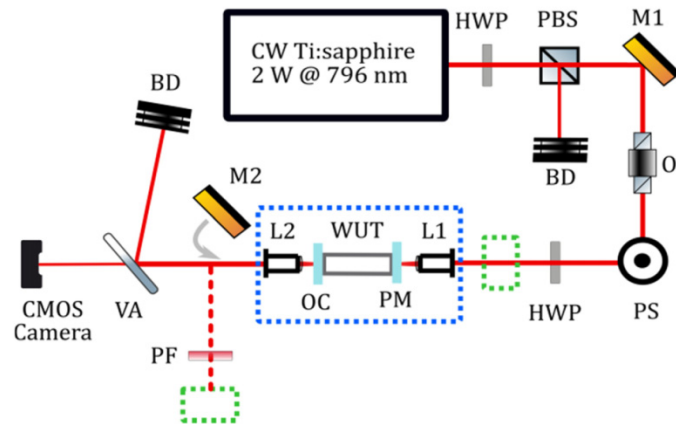


Fig. 2. Waveguide laser experimental setup. HWP, half-wave plate; PBS, polarizing beam splitter; BD, beam dump; M1 and M2, gold mirrors; OI, optical isolator; PS, periscope; L1 and L2, AR-coated aspheric lenses; PM, pump mirror; WUT, waveguide under test; OC, output coupler; VA, reflective variable ND filter; PF, optical filter. Blue dotted box signifies components mounted on waveguide alignment workstation. Green dotted box signifies power meter or detector positions.

In this configuration the pump light was coupled into each waveguide in the array in turn with the alignment checked at low power using an aspheric lens (L2) to image the waveguide end facet onto a CMOS camera sensor. The fluorescence emission from each of the $\text{Tm:Lu}_2\text{O}_3$ waveguides was monitored using an unbiased photodetector (Thorlabs DET10D, 1.2 – 2 μm) after a filter providing >40 dB of attenuation at the pump wavelength. The fluorescence signal was maximized by tuning the cavity alignment and input coupling of the pump light and a check for a lasing threshold was then undertaken by increasing the pump power. In all the waveguides tested only the structures written with 2 μJ and 3 μJ energy pulses and 30 μm track separation exhibited lasing with the best performance observed from the 2 μJ written structure. No waveguides were written with pulse energies between 2 – 3 μJ and so further exploration of waveguides written with pulse energies in this region is justified to see if improved performance can be attained.

With the waveguide emitting the highest laser output in the array established, the output power vs input pump power characteristics were measured with the range of OCs [Fig. 3(a)]. For these measurements two power meters (Thorlabs S310C) were used to measure the input pump power and emitted signal at the positions shown in Fig. 2. Using the known losses at the signal wavelength for the optics downstream of the output coupler the output power emitted from the waveguide could be calculated. The absorbed pump power was determined by measuring the residual pump power transmitted through the OC with the pump filter removed and the signal power subtracted, and using this to estimate a conversion factor to calculate the absorbed power from the input power. For such conversion from the measured incident power to absorbed, a perfect coupling of the pump signal into the waveguide was assumed except for a single Fresnel reflection due to the uncoated end facets (i.e. no coupling loss due to mode field mismatch between the guided pump mode and the pump spot profile). This assumption gives conservative (higher) values for absorbed pump power due to

uncertainties in calculating the coupling loss into the waveguide. A maximum output power of 81 mW was generated using the 40% output coupler for an absorbed power of 1.18 W, as shown in Fig. 3(a). In addition, under optimal alignment conditions with the 40% output coupler a maximum slope efficiency of 9.5% was attained. However, a lower output power of 52 mW was generated at such conditions due to the presence of a slight degradation of the pump laser output at the time of achieving this result.

Across the series of output couplers tested, thresholds were observed to be in the range of 50 - 200 mW and the lasing emission spectrum remained centered around 1942 nm as measured using a fiber coupled optical spectrum analyzer (Thorlabs OSA205). From the slope efficiencies calculated for each output coupler a modified Caird analysis [21] was performed in order to determine the parasitic round trip loss for the signal wavelength in the cavity, which due to cavity design, we equate to the round trip propagation loss for the waveguide. The Caird analysis uses the relationship between the measured slope efficiencies (η_s) and the known output coupling (T_{oc}) to determine the cavity losses (L , per pass). However, it should be modified to contain logarithmic arguments in the case of large T_{oc} and L :

$$\frac{1}{\eta_s} = \frac{1}{\eta_0} \left(1 + \frac{2\gamma_i}{\gamma_{oc}} \right) \quad (2)$$

$$\gamma_i = -\ln(1 - L) \quad (3)$$

$$\gamma_{oc} = -\ln(1 - T_{oc}) \quad (4)$$

where η_0 is the limiting slope efficiency, γ_i is the logarithmic internal loss of the cavity per pass and γ_{oc} is the logarithmic loss of the output coupler.

Fitting the above function to the measured slope efficiencies data [Fig. 3(b)] the propagation losses at the signal wavelength for the lasing waveguide were estimated to be $0.7 \text{ dB}\cdot\text{cm}^{-1} \pm 0.3 \text{ dB}\cdot\text{cm}^{-1}$.

The near field mode profiles of the pump and lasing signals at the output facet of the waveguide were imaged using commercial visible (Thorlabs DCC1545M) and mid-IR cameras (FLIR SC7600M), respectively. The pump mode was imaged directly onto the camera sensor whereas the lasing signal mode was imaged onto a screen through the pump filter, and subsequently viewed with the IR camera. The waveguide structure demonstrated multimode characteristics at the pump wavelength of 796 nm but single mode propagation was observed at the laser wavelength, as shown in Figs. 4(b) and 4(c). This behavior indicates that there is not ideal overlap between the pump and signal modes and hence pumping at longer wavelengths (in-band pumping) might provide further improvements to the laser slope efficiency due enhanced mode matching. A Gaussian fit of the lasing mode was performed using a scaled image containing a calibration target, this gave the mode field diameter ($1/e^2$ level) of signal of $22.5 \text{ }\mu\text{m}$ and $25.2 \text{ }\mu\text{m}$ in the x and y directions, respectively [Figs. 4(d) and 4(e)].

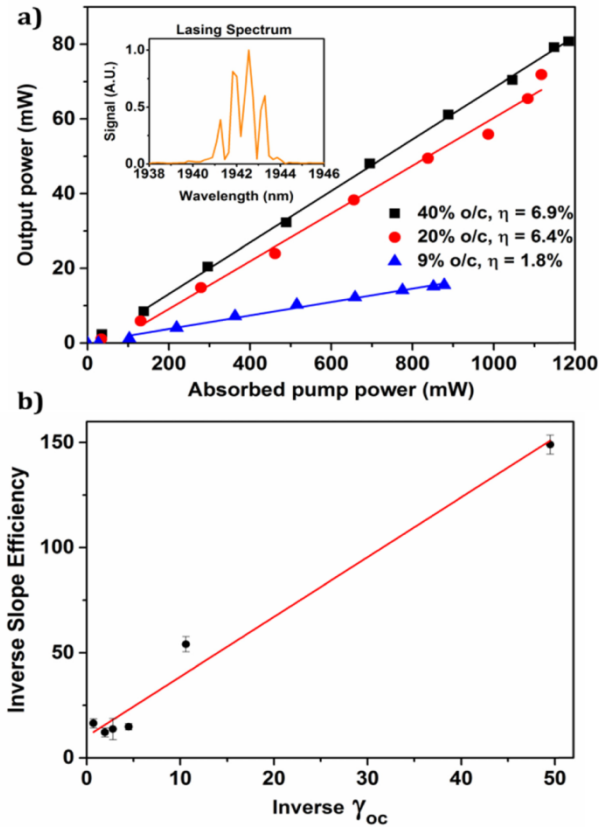


Fig. 3. (a) Input-output power characteristics of the Tm:Lu₂O₃ waveguide laser with different output couplers at the maximum output power experimental conditions. The inset shows the laser spectrum. (b) Experimental data and a linear fit of the inverse measured slope efficiencies against inverse output coupling.

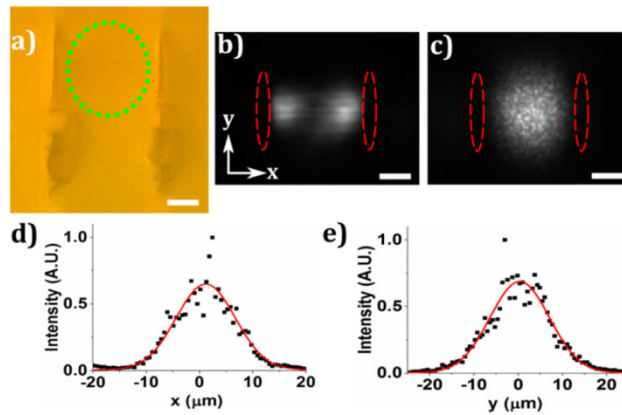


Fig. 4. (a) Microscope image of the waveguide used in the laser experiments. (b) and (c) show the pump (796 nm) and the laser (1942 nm) mode images, respectively. 10 μm scale bars are included. The green dotted circle shows the unmodified guiding region. Red dashed ellipses indicate the area of the inscribed tracks. (d) and (e) are the Gaussian fits to slices through the laser mode image in x and y directions, respectively.

To investigate the waveguide losses at the pump wavelength a modified version of the setup described in Fig. 2 was used. This involved the removal of the cavity mirrors and pump filter used for laser experiments and a detuning of the Ti:sapphire pump laser to a wavelength of 860 nm where there is a negligible absorption by the Tm:Lu₂O₃ sample. Incident and transmitted power measurements were taken with optimal coupling into the waveguide used in the laser experiments. In addition, a background loss value was taken by measuring the incident and transmitted power for just the lenses used by translating the sample out of the beamline to ensure that no clipping of the pump laser beam had occurred. These results allow for the calculation of the insertion loss for the laser waveguide at the pump wavelength which was estimated to be 1.6 dB. With the insertion loss established at the pump wavelength, measurements of the propagation loss of the waveguide allow for extraction of the coupling efficiency. However, the multimode nature of the waveguide at the pump wavelength inhibits the use of the most prevalent methods for accurate propagation loss measurements and thus the coupling loss could not be accurately determined.

4. Conclusion

In conclusion, we have demonstrated the first waveguides in Tm³⁺-doped Lu₂O₃ ceramics fabricated via ULI. Waveguide structures were written utilizing various pulse energies and track separations and a transition from Type I to Type II guiding was observed as pulse energy increased. Lasing from a microchip Tm:Lu₂O₃ waveguide laser was achieved with a maximum output power of 81 mW at 1942 nm and a slope efficiency of 9.5% was measured. Thresholds were observed to be in the range of 50 – 200 mW across the range of output couplers tested. Waveguide losses at the emission wavelength were found to be $0.7 \text{ dB}\cdot\text{cm}^{-1} \pm 0.3 \text{ dB}\cdot\text{cm}^{-1}$. The occurrence of Type I guiding indicates the possibility of ULI waveguide writing in Tm:Lu₂O₃ ceramic using a method optimized for this regime such as multiscan inscribing which has been shown to be a route toward low threshold and high slope efficiency waveguide lasers in other gain media [22]. Furthermore, the writing of depressed cladding waveguide structures in Tm:Lu₂O₃ is also feasible as it has been established for other mid-IR gain media [8]. This highlights the potential of Tm:Lu₂O₃ for further development of high power and efficient waveguide lasers around 2 μm and such opportunities will be fully explored in future work.

Funding

UK Engineering and Physical Sciences Research Council (EPSRC) (EP/G037523/1, EP/L01596X/1).

Acknowledgments

The Authors would like to thank Photonic Solutions Ltd. (Heriot-Watt University Research Park, Edinburgh, UK) for providing the inscription laser used in this work and Professor Alan Kemp (IOP, University of Strathclyde, Glasgow, UK) for use of the mid-IR camera. J. Morris and N.K. Stevenson acknowledge the EPSRC Centre for Doctoral Training in Applied Photonics and Fraunhofer UK for studentship funding.